Virtual screening and cheminformatics descriptors uncover insecticidal molecular mechanisms besides plant essential oils' action.

Eduardo José Azevedo Corrêa
Minas Gerais Agricultural Research Company (EPAMIG)
Frederico Chaves Carvalho
Federal University of Minas Gerais
Júlia Assunção de Castro Oliveira
Federal University of Lavras
Suzan Kelly Vilela Bertolucci
Federal University of Lavras
Marcus Tullius Scotti
Federal University of Paraíba
Carlos Henrique da Silveira
Federal University of Itajubá
Fabiana Costa Guedes
Federal University of Itajubá
Júlio Onésio Ferreira Melo
Federal University of São João del-Rei
Raquel Cardoso De Melo-Minardi
Federal University of Minas Gerais
Leonardo Henrique Franca de Lima (leofrancalima@ufsj.edu.br)
Federal University of São João del-Rei

Article

Keywords: Computational biology, virtual screen, essential oils, Baccharis dracunculifolia, blowfly

Posted Date: November 11th, 2022

DOI: https://doi.org/10.21203/rs.3.rs-2223409/v1

Additional Declarations: No competing interests reported.

Version of Record: A version of this preprint was published at Scientific Reports on March 21st, 2023. See the published version at https://doi.org/10.1038/s41598-023-29981-3.

Abstract

Plant essential oils (EOs) are important for discovering new bioactive substances, such as environmentally safe insecticides. However, the high structural diversity of EOs compounds and their elusive biochemical mechanisms make a gap in knowledge of their major targets and action mechanisms. Here we present a predictive cheminformatics methodology and experimental validation of the ability of EO's typical natural compounds to act as potential insecticides against canonical insect molecular targets. A cheminformatics analysis protocol was created to identify chemical signatures of compounds present in EOs capable of interfering with typical targets of insecticides. Three of our clusters presented strong respective signatures for JH-like, Steroids-like and biogenic-amines-like structures, all of them with reported anti-insecticidal effects. Case studies highlight the participation of juvenile hormone-specific proteins (JHBP and MET) and the octopamine receptor at agonist conformation (OctpR ago) as major targets for EOs of typical Brazilian plants. *In vivo* application of leave's EOs from *Baccharis dracunculifolia* on blowflies led to dose-response symptoms in adults, larvae and hatching consonants with such signatures. Taking it all together, the present study points out the success of a promising methodology to identify insecticidal pharmacophore signatures on plants' EOs, which can be of high value for the bioprospection of new natural products and molecules with agro and health interests.

Introduction

Essential oils (EOs) are plant secondary metabolites physiologically important for signaling, pollinator attraction, allelopathy, adaptation to abiotic stresses and defense against herbivores and pathogens. They are natural agents used for their many biological properties [1]. Their applications in agriculture have been the object of research for several decades, with uses as antifungal, antibacterial, weed control products and natural eco-friendly insecticides [2]. The use of EOs in pest control has two advantages: first, their low toxicity on mammals, birds and fish, which translates into safer products and second, the great structural diversity of their components, making them a potential source of multi-target bioactive molecules [2].

Some insect receptors share the literature-reported behavior as targets for current commercial pesticides and EOs compounds. The most related targets for insecticides are of neurochemical/neurohormonal nature: the acetylcholinesterase enzyme (AChE) [3], which degrades the neurotransmitter acetylcholine; neurotransmission regulators such as the γ-aminobutyric acid receptor (GABAaR) [4] and the Octopamine receptor (OctpR) [4]. Other studied targets for commercial insecticides and EOs are Insect Growth Regulators (IGRs), which affect the timing of molting during insect metamorphosis, particularly the Methoprene-tolerant receptor (MET), being this the physiological receptor of the juvenile hormone (JH); the Ecdysone hormone receptor (EcNR) [5, 6]. Besides MET, the JH pathway is also targeted indirectly by enzymes involved in its synthesis and degradation, as well as crucial transporters for this molecule. This last case highlights the juvenile hormone binding protein (JHBP), whose action is reported to be paramount in the adult's reproductive cycle [7].

The AChE (Fig. 1A) is responsible for neurotransmission in insect neurons. Inside the synaptic cleft, this enzyme breaks acetylcholine into choline and acetyl, interrupting the nervous system's electric impulses [13]. Its inhibition causes acetylcholine accumulation resulting in fatal nervous system overstimulation, and consequently, this is widely targeted for common insecticides [14, 4]. The ionotropic γ-aminobutyric acid receptors (GABAaR) act in insect neurotransmission in both central and peripheral neural systems (Figs. 1B and 1C). This is a channel membrane receptor involved in the neuron hyperpolarization process that promotes muscle relaxation and other functions [4, 12]. Insecticides like Abamectin act as agonists (Fig. 1B), causing lethal nervous system inhibition [12]. Whereas insecticides like dieldrin and fipronil act as antagonist inhibitors of the GABAaR (Fig. 1C), causing a fatal overexcitation of the insect nervous system [5]. There are limited data on the EOs' effects on this target, but it is reported that monoterpenes can increase GABAaR-mediated chloride uptake and allosteric modulation in insects [4].

The insect octopamine receptor (OctpR) is a G-protein coupled receptor (GPCR) class (Figs. 1D and E), which is a canonical target for the prospection of insecticides [12, 15]. Octopamine (Octp) is the natural agonist, and its antagonists like Epinastine (Epin), act as a neurotransmitter, neurohormones and neuromodulators [4]. In insects' physiology, this Octopaminergic system modulates muscle activity by directly acting on muscle fibers, changing the basal tonus [16]. In the sensory system as antennae, halteres and wings, the octopaminergic system increases the activity of olfactory neurons, attractive stimuli odor, pheromones and nestmate recognition, auditory frequency tuning and mating behavior [15]. And it is responsible for inducing oviposition in adult female flies [17]. Recent reports also show that OctpR is involved in metamorphosis both through the inhibition of the Juvenile hormone (JH) biosynthesis in insect *Corpus Allatum* (CA) or by enhancing ecdysone synthesis at insect prothoracic glands (see below) [18]. EOs and other phytochemical compounds are reported to interact with insect Octopamine receptors (OctpR), mainly as agonists (OctpR/ago), Figure D [4].

Larval development and metamorphosis are controlled mainly by a pair of ligand-responsive transcription factors: Ecdysone nuclear receptor (EcNR) and Methoprene tolerant protein (MET), Fig. 1F and 1G, respectively [5, 19]. The EcNR is a nuclear superfamily receptor [6, 19] that is triggered by ecdysteroid hormones (EcH) [6, 19]. This protein coordinates events such as insect molting and metamorphosis transitions to adult form. The binding of an agonist compound causes the heterodimerization with another nuclear receptor, the Ultraespiracle, and initiates a genetic transactivation cascade leading to the molting and change of life form [19].

On the other hand, Juvenile hormones (JHs) are important insect hormones that retain the larva in the juvenile state. Substances able to interfere in metamorphic signaling are potential sources of insecticides once this process is absent in vertebrates' metabolism. Plants in nature explore this feature to avoid herbivores. The presence of EcHs or JHs analogous substances on EOs can mimic the natural hormones and naturally control plague infestation [4, 12]. Juvenile Hormone Binding Protein (JHBP), Fig. 1H, is a juvenile hormone carriage protein, present only in pupae and adults, transporting JH through the hemolymph and protecting it from degradation [7]. This protein is essential in ovary maturation and the normal reproductive behavior of adult insect males. Recent reports highlight its function in the insect's

immunity and hematopoiesis [20]. In addition to the fact that we do not have commercial insecticides for this target, it is an important target for developing safe insecticides once it is not present in vertebrates' metabolism.

Investigating how the many components of essential oils affect these molecular targets may be the key to understanding why some EOs exhibit insecticide and larvicide properties. This understanding can also highlight some l symptoms and results arising after EOs bioassays with insects. Besides the large body of experimental evidence suggesting these EO's properties, little is understood about their biochemical mechanisms of action [4]. To fill this gap, computational methods are promising tools that can supplement experimental knowledge, providing a better understanding of how natural compounds act in biological systems [8]. A set of studies demonstrate the efficacy of virtual screening and cheminformatics in identifying promising molecules for desired biological functions [9] or as a starting point to guide experimentation. Also, computational data mining methods are increasingly common in biological studies and have successfully identified and even proposed novel ligands for molecular targets of interest [10].

This study proposes a computational pipeline to understand how plant EOs compounds might affect insect physiology. This protocol combines comparative structural modeling techniques, virtual screening using molecular docking, quantitative structure-activity relationship (QSAR) descriptors and data mining algorithms to identify the signature of natural molecules that can act as insecticidal or larvicidal. The principle of this protocol is to use the molecular similarities, measured by metrics like Tanimoto and chemical space Euclidean distances [8], to estimate the interference of compounds present in EOs obtained from plant species on key protein targets of insects. Our method reveals that several tested compounds have a significant signature with the studied targets, indicating their potential as bioactive ingredients for natural pesticides.

To test the hypotheses from our initial computational findings, we conducted a case study evaluating the insecticidal and larvicidal potential of the *Baccharis dracunculifolia*'s EO against the *Chrysomya albiceps* (Wiedemann, 1819) blowfly, Calliphoridae. This insect species from the Calliphoridae family is responsible for causing myiasis, a concerning disease that commonly affects cattle. It causes wounds in the animal body, resulting in important reductions in weight gain and milk production potential. In Brazil, this disease is estimated to be responsible for millions of dollars in losses annually [11]. We hope the results and the methodology provided here will be valuable to add more predictability to the study of the EOs' actions and their biotechnological potential; as well as to improve the search for new efficient, and environmentally friendly natural compounds for agriculture, medicine, industry, technology and scientific ends.

Results And Discussion

Cluster archetypical signatures as predictors for the binding potential to different targets

After all molecular docking experiments had been performed, the 1% top-scored ligands from all docked ligands for each of the eight blowfly biochemical protein targets were determined, resulting in a subset containing 46 top hits ligands. Then the Tanimoto coefficient and hierarchical clustering were used to establish clusters of molecular similarity based on the Tanimoto similarity metric (1-Tanimoto Coefficient). The established molecular cluster is presented in Fig. 2 and Figure S10. In Fig. 2, the bar heights represent the number of protein targets affected by each ligand. Almost all ligands have a unique target protein, but clusters D, E and J are formed by undiscriminating ligands that bind to six blowfly targets. Clusters are composed, in the majority, of Sesquiterpenes, being of aliphatic (Clusters A, G, H) or alicyclic nature (Clusters C1, C2, C3, C6, H).

The different clusters determined have well-established chemical signatures. These signatures are detailed in Table S9. Cluster A are sesquiterpenes compounds formed by an open chain with three isoprene units. The sesquiterpenes are reported as repellent and insecticidal agents that cloud be used in pest control [27]. Their skeleton resembles the chemical topologies of the Juvenile Hormones, the natural ligand of the JH receptor. EO compounds like E-Nerolidol (Cluster A) are reported for insect repellency, larval mortality, and ovicidal activity [28]. A recent study applying E-Nerolidol on Egyptian cotton leaf worms indicates that this sesquiterpene can produce strong larvae toxicity, reducing larval weight gain, prolonging the pupal and larval duration, a dose-dependent pupation inhibition and pupae malformation [29].

Clusters B, C2, C9, C10 and D are diterpenoid compounds with four rings of carbons in Clusters B and C9. Keto lactone is represented in Cluster F. The Clusters C1, C5, C7, G, and I show a chemical signature of compounds with one ring of carbon coupled with an aliphatic chain (Figure S10).

Diterpenes from cluster B with Phytosteroid architecture (presenting a carbonic skeleton like Phenanthrene with 3 C6 rings connected). In this way, they are structurally similar to the Ecdysone Insect Hormone structure. As shown in Matrix 1 in Fig. 3, these Diterpenoid clusters (C9 and D) have a significant signature to the Ecdysone receptor. Literature relates several abnormalities associated with premature metamorphosis (an ecdysone agonist action) on the larval treated with diterpenoids isolated from EOs capable of assuming Phytosteroid-like topologies [30].

Sesquiterpene Lactones are represented in Cluster C6. They all have structure variations but with three oxygen in the chemical structure. Sesquiterpene Lactones are relatively well-documented insecticidal and antifeeding activities for insects [31].

Cluster G presents skeleton topologies like biogenic amines like dopamine and octopamine (without nitrogen atoms and with relatively smaller aliphatic side chains than these amines). Cluster G and biogenic amines show benzene radicals in the *para* position and an aliphatic chain marking position 1 in the benzenic ring. Octopamine and compounds in Cluster G are more topologically related because of the aliphatic lateral chain branching on the first carbon. Dissimilarities between the terpenoids and the biogenic amines are the oxygenation pattern, the length of the lateral chain and the presence of nitrogen in biogenic amines.

As it could be inferred from the computational analysis, compounds with similarities with cluster G are probability agonist signatures to the Octopamine receptor (see Matrix 1 in Fig. 3). Cluster G is formed by sesquiterpenes with an organic skeleton topologically similar to biogenic amines such as octopamine, besides there is no amine group in its skeleton. Therefore, the higher fitting of compounds from this group to the OctpR at the agonist conformation is a consonant issue.

High-chain aliphatic compounds like phytol and 9-Octadecyne of cluster J showed promiscuity for targets (Fig. 2 and S10). This is probably because its chains are easily entangled in multiple configurations and associated with different protein binding sites. Phytol strikes the insect nervous system and causes neurotoxic effects through several mechanisms by inhibiting AChE activity [32, 33, 34, 35], agonist effects like benzodiazepines, producing sedative and anxiolytic activities the GABAa receptor [36, 37], and agonist of octopamine receptors [38].

It is reported that phytol alters the normal pattern of insect growth and development patterns. A prolonged larval duration when treated with retinol and phytol, a prolonged larval duration indicates larval tendencies to retain their larval stage [39]. However, the biochemical mechanisms by which these effects happen remain unclear.

Predicting of EOs’ action on blowfly protein target

The first matrix produced, named Matrix 1, is shown in Fig. 3 and represents the number of compounds belonging to each hierarchical cluster high-scored in virtual screening to bind to each blowfly protein target. In other words, it represents the probability of the hierarchical cluster compounds being highly scored for each target.

The second matrix, matrix 2 in Fig. 3, represents the fraction of the compound high scored in virtual screening for each blowfly protein target that belongs to each hierarchical cluster. In other words, this represents the specificity degree of each protein target for the chemical clusters determined. Considering the values obtained in these results and shown in matrix 2. Antagonists of the GABA receptor (0.44 in cluster B) and octopamine receptor (0.5 for cluster C2) are supposed to be most restrictive to chemical features of compounds present in EOs’.

Matrix BDSTFL is the Molecular Similarity matrix of Degrees of Belonging calculated based on the Tanimoto coefficient determined by Fuzzy Logic determined by the degrees of belonging to the clusters obtained by hierarchical clustering. Read the methods section o see about calculations. And Matrix EPNMCS contains normalized Euclidean proximity of EOs compounds from the 0.1% hits archetypical ligands to each blowfly protein target. This matrix was named the Euclidean Proximity Normalized Matrix to Cheminformatics Space vectors and is calculated as described in the methods section.

A pairwise correlation considering the average of docking score rank and, respectively, the multiplication of Matrix 1 and Matrix 2 (Fig. 3) multiplied by matrix EPNMCS and matrix BDSTFL was performed to validate the molecular similarity metrics approach. The correlations are shown in Fig. 4; letters A and B

show the correlation considering the similarities calculated considering the Euclidean metric based on molecular descriptors. Moreover, letters C and D are pairwise correlations considering the topological Matrix based on Tanimoto similarity.

The strongest correlation between docking scores and distances obtained from Euclidean metrics can be observed using molecular descriptors, $r^2 = 0.276$ and $F = 48.069$. Therefore, based on these achievements, we consider for further analysis only the Matrix of target versus EOs compounds generated by multiplication matrix of probability to affect each target (matrix 1, in Fig. 3) and Euclidean proximity of each EO compound to hierarchical cluster based on the z-scored molecular descriptor (matrix EPNMCS).

To determine and visualize the behavior of rank points in y ordinate along the measurement parameter for chemical similarity measured by fuzzy logic or QSAR descriptors in abscissa x, we split the abscissa values into categorical classes of 0.1 bins and proceed with an Analysis of Variance (ANOVA) with post hoc mean comparison by Tukey test. Following this procedure, we can construct the Bar plots shown in Fig. 4.

It can be observed in the bar plots shown in Fig. 4 that, statistically, the use of BDSTFL did not return predictable information of rank score in docking of plants EOs. On the other side, if it is considered the EPNMCS metrics, especially when the EPNMCS matrix is multiplied by the matrix of the probability of the hierarchical cluster affecting each target (Fig. 4A - Matrix 1). It is possible to observe the separation into two discrete categories: low Euclidean proximity and low docking scores (indicated by the letters a and b), and proximities values higher than 3.01 z-scores featuring high docking scores (letter c).

This statistical information allowed us to build a likelihood Matrix (Fig. 5A), considering values higher than 3.01 have a high probable signature to the protein target, which is a donated value of 1.00. Otherwise, proximity classes with values lower than 3.00 are labeled with zero.

Using this likelihood matrix, we initially selected five plant species to predict the action of plant EOs on the blowfly molecular targets. Three of the species belong to the Asteraceae family (*Baccharis dracunculifolia*, *Baccharis retusa* DC. and *Disynaphia spathutata* (Hook. & Arn.) R.M. King & H. Rob) [40]. Furthermore, the other two species are *Myracrodruon urundeuva* Allem. (Anacardiaceae) and *Callistemon viminalis* (Sol. ex Gaertn.) G. Don (Myrtaceae) was already being worked on by our research group [41, 42].

The prediction of actions was calculated by multiplying the likeliness matrix (Fig. 5A) and the EOs compounds fractions determined from the Profile of Gas Chromatography (Table S6 and published studies [41, 42]), resulting in prediction scores in Fig. 5B, which is the degree in z-scores of Euclidean proximity of species EOs concerning each molecular blowfly target. High values in Fig. 5B greater the degree of influence of EOs on blowfly molecular targets.

It is possible to observe that compounds in EOs have high chemical signatures as agonists for the Octopaminergic system, MET Receptor and JHBP protein. These computational results (Fig. 5B) suggest

that plant species' EO act mainly as an agonist of the Octopaminergic system and as a juvenile mimetic hormone with a signature to Methoprene Tolerant bHLH–PAS receptor (MET) and Juvenile Hormone Binding Protein (JHBP). It is possible to see that the mainly predicted influence is the OctpR agonist over the PAS Methoprene Tolerant Receptor (MET). The strongest predicted agonist action for OctpR was obtained for *Myracrodruon urundeuva* EO (1.9 see Fig. 5B).

The specific chirality of EOs compounds can determine stereochemistry dependence for insecticidal activity [43]. However, Cluster's chemical signatures of high-scored compounds to biochemical blowfly targets are robust enough to allow us to calculate metric similarities and compare EOs compound chromatograms from different species.

Case study: EO applied on Myiasis-producing blowfly

Aiming a case study to provide the first experimental validations of the signatures predicted by our methodology, we carried insect dose-response assays for the EO extracted from *B. dracunculifolia* leaves (whose chromatographic profile was submitted to our methodology, resulting in the profile predicted in Figure Bm *top* line). These bioassays, in turn, were carried against the blowfly *Chrysomya albiceps* (Calliphoridae) [44]. *C. albiceps* is a blowfly commonly found in poultry house production and other Calliphoridae flies with health relevance. The application of EO from *B. dracunculifolia* was chosen based on bioassay results already published [45], high species frequency in all-natural areas [40] and sufficient EO production per gram of fresh leaves (~ 1mL per 150g).

In fumigant bioassay on adult blowfly *C. albiceps*, the Kaplan-Meier survival curves, presented in Fig. 6A, and the log-Rank test points out a significatively enhanced kill of adult flies after the application of doses higher than 10%. The 30% of *B. dracunculifolia* EO application significatively has the highest adult blowfly killer action.

A few minutes in contact with EO, it is possible to see a high-frequency vibratory flapping wing (Observational data) and, after 22h, high oviposition of immature eggs (Fig. 6B). Li et al. (2020) report octopamine-induced oviposition via both α and β octopaminergic receptors in *Plutella xylostella* (Linnaeus, 1758) [17]. Flight muscles are innervated by neurons containing the Octp receptor, and a published report states that octopamine is involved in insects' fast-flight muscle excitation [46]. The Octopaminergic system establishes the octopamine-induced rhythmic motor pattern. It has been demonstrated that applying the Octp antagonist deafferents flight system on locusts (*Locusta migratoria*, Linnaeus, 1758) leads to a wingbeat frequency decrease [15]. These first visual observations of premature oviposition and high frequency of flapping wings with *B. dracunculifolia* assays are, hence, in consonance with the *in silico* predicted high potential for Octopaminergic agonism in Fig. 5.

In Toxicity Bioassay, Larvae motility measured by the frame-by-frame cosine distance video technique, as described in the Methods section, shows a dose-dependent behavior (Videos in V1) presenting a cyclic or periodic response of larvae motility to EO concentration applied. It is possible to see three motility peaks with positive feedback reinforcing loops (Fig. 6C and Fig. 7F). Cyclic biochemical responses to

octopamine levels in insects play a critical role in the circadian control of olfactory transduction, and pheromone detection thresholds daytime-dependently mediate, signals in olfactory learning, memory, circadian rhythms of sleep and activity, juvenile hormone biosynthesis, and the response characteristics of optic flow processing neurons in the fly's visual system [47, 18, 48]. Therefore, the insect octopaminergic system plays an important role in the circadian or periodic biochemical insect. And in this regard, the ability of EOs compounds to elicit an agonist response by the OctpR receptor could elicit a cyclic response in larvae motility, as observed in Figs. 6C and 7F.

Octopamine (Octp) is the invertebrate norepinephrine-analog, and its physiological effects are related to the "fighting or flight" response. The application of octopamine creates a dose-dependent twitch increase in Australian cricket [49] and contraction amplitude in various arthropod species [16]. Predicted by *in silico* analysis (Fig. 5B) and observed in bioassay (Fig. 6C and 7F), the application of EOs on *C. albiceps* larvae shows concentration-dependent like as that observed by Thompson et al. (1990) studying the agonism in the Octopaminergic system of cockroach.

The CA is a high-innervated gland in the insect central nervous system (CNS) [50]. It is largely recognized that CA and JH biosynthesized has a crucial role in insect Metamorphosis, sexual maturation, and reproductive physiology [51]. Octopamine (Octp) modulates many peripheral and sensory organs and, in the nervous system, exerts an inhibition effect on juvenile hormone biosynthesis in a sinusoidal dose-dependent reversible manner [18]. This phenomenon is well documented in cricket and cockroaches, and this biochemical mechanism seems to work on flies [52].

Larvae motility is controlled by the Octopaminergic system [15, 16, 49], and we can see that EO concentration stimuli an agonist of OctpR in a cyclic pattern like that observed by Thompson et al. (1990) in inhibition of JH biosynthesis. When low EO concentration is applied to blowflies, it stimulates the Octopaminergic system. It increases larvae motility at 10% (point 3 Fig. 7F), which is reversed between 13–15% (points 4 and 5 Fig. 7F). An enhanced motility loop starts again at 13% EO concentration, which increases to a peak concentration of 18% (points 4 to 6 in Fig. 7F), and the last high motility peak reaches 30% (point 9 in Fig. 7F). Therefore, we can conclude that the cyclic pattern of larvae motility observed in the bioassay is a consequence of an Octopaminergic system response like that observed by Thompsons et al. (1990) when applied different agonist concentrations, in our case, the EO compounds.

Applying *B. dracunculifolia* EO on the last instar larva causes a sharp decrease in the pupal formation rate (Fig. 6D). The insect metamorphic process is controlled mainly by Ecdysteroid hormones that trigger the insect to molt and Juvenile Hormone, which maintains the youth larvae feature until the right moment for pupae formation.

The EO *B. dracunculifolia* has a strong cheminformatics signature against the MET receptor, decoding a biological signal to delay pupae formation between 5% and 13%. Concentrations above 15% restore the pupal formation rate, like the control group. However, the pupae formed in this treatment have decreased volume (Fig. 6E) and increased the number of adults deformed (Fig. 6G). A decrease in the length and diameter of pupae is only observed at the same time as the second peak in larvae motility (point 5 in

motility plot Fig. 7F). When a high concentration is applied, a proportional increase of adults hatched with deformities is observed (Figs. 6G and 6H).

Based on the computational and Bioassays results, it is possible to infer that *B. dracunculifolia* EO exerts an agonism effect on the octopaminergic system, evidenced by the cyclic in larvae motility over different EO concentrations. Agonism to Octp leads to JH biosynthesis suppression by larvae CA, which breaks the downregulation promoted by the Krüppel-homolog 1 (Kr-h1) transcription factor, which would provoke a change in the timing of the larval metamorphosis, causing malformation and adultoid death at hatching [53].

Low levels of JH trigger the biochemical process that leads to the pupae phase, as observed by the increase in pupae rate formation, increase in adults hatched dead and deformed and decrease in pupae volume at concentrations between 13–20%.

Adult deformities on blowflies *Cochliomyia macellaria* (Fabrício, 1775) at hatching were also reported by Chaaban et al. (2018) after applying crude EO's *Baccharis dracunculifolia*. Deformities observed by these authors include small size, malformation, poor development, deformed wings and legs, and dried pupae [45] and reported by Khater et al. (2013) applying crude EOs in *Lucilia cuprina* (Wiedemann, 1830) [54]. Cockroaches' nymphs treated with juvenile hormone mimic compounds died with intact old cuticles, showing an inability to complete the molt. A small percentage hatched, not fully leaving the old cuticle and eventually died [53]. Molting disruptions were observed after applying excessive amounts of Juvenile hormone or its analogs in *B. germanica*, displaying several abnormal characteristics, including twisted wings and improper sensory organs [53].

The metamorphosis is the passage of larvae to adult form. From the hormonal point of view, the Juvenile Hormone (JH) produced in insect CA plays an essential role in many aspects of insect physiology. In larvae life, the JH action acts throughout the receptor PAS Methoprene-tolerant (MET) that heterodimerizes with another bHLH-PAS protein Taiman (Tai) and activates the transcriptional factors Krüppel-homolog 1 (Kr-h1), maintaining the larval form [52]. Aliphatic sesquiterpenes present in EO compounds are JH-mimetic which can bind in Methoprene-Tolerant receptor (MET), as denoted in computational prediction Fig. 5B, which can be responsible for the delay in pupal formation rate between 5–13% concentration.

The JH in metamorphosis maintains the immature condition, and the progress to pupae-adult insect form will occur in its absence at the end of larval life. Allowing the larvae to molt to pupal form and JH still absent in most pupal life allows the formation of an adult at the next molting [53]. Deficiency in JH promotes precocious metamorphosis and pupal lethality by suppressing the zinc-finger TF Krüppel-homolog 1 (Kr-h1), which acts as the anti-metamorphosis factor [52]. The incorrect JH levels and timing will deregulate the larval-pupal-adult formation. Kr-h1 suppression in the late instar stage induces precocious metamorphosis and adultoid formation, like EOs application [55].

Pearson correlation of Larvae Motility (M), Rate of Pupae Formation (PR), Pupae Volume (V) and Number of adults Dead and Deformed at hatch (D&D) and EO concentration (EO_C) is presented in Fig. 7. We can observe a positive correlation between D&D and EO_C. In other words, the increase in EO concentration will result in more adults deformed and dead. And a negative correlation between V and EO_C or an increase in EO concentration will result in a decrease in pupae volume (Fig. 7A to 7E).

Changes in M are biologically attributed to stimulation of the insect octopamine system [15, 16, 49], considering the average Pearson correlation of Laval motility with EO_C of 0.67, with V of -0.58, and with D&D of 0.55. We can infer that the OctpR receptor stimulation by increasing the concentration of essential oil is directly related to the reduction of pupal volume and the appearance of deformed and dead adults at the end of Calliphoridae flies' metamorphosis.

It is interesting to note that at low EO concentrations, it is possible to observe a marked negative correlation (-0.84) between the pupation rate (PR) and EO concentrations of 0 to 13% at the first peak of larval motility (Fig. 7B and 7F) and that changes drastically change to a positive correlation (0.9) at EO concentrations of 13 to 20 (Fig. 7C and 7F) corresponding to the second peak of larval motility. But, on average, it shows almost no correlation with EO_C. We can understand that *B. dracunculifolia*'s EO possesses compounds with strong chemical signatures that function as MET receptor agonists, which promote a delay in PR, and compounds with strong signatures as OctpR agonists inhibiting the biosynthesis of the JH. Therefore, the *B. dracunculifolia* EO seems to work as a balanced system, at low oil concentrations, especially by the high composition of a sesquiterpene with a signature for the juvenile hormone, the E-nerolidol, the agonist action of the MET receptor stands out. And it will result in a PR delay observed between concentrations of 5 to 13% of EO (Fig. 6D). But suppose we start to increase the EO_C application enormously. In this case, it will increase compounds with an agonist signature to the OcptR and will induce a dramatic drop in the concentration of JH, increasing the pupation rate (PR) observed in Fig. 6D.

When we slice the motility plot in the increasing phase of the second peak (points 4-5-6-7 in Fig. 7F), which correspond to concentrations between 13–20%, the larval motility at these points strongly correlates with pupae rate formation (0.96 Fig. 7C), perfectly fits with a fraction of adults hatched dead and deformed (1.00 Fig. 7C) and is inversely correlated with pupae volume (-0.99 Fig. 7C). It is hard to believe these strong relationships are due to mere chance.

The computational protocol used here helps us to understand the biological phenomena besides the EO's action in insect metamorphosis. The agonist effect of compounds present in EOs can suppress the biosynthesis of JH by CA through the Octopamine receptor, which will increase pupation rate and decrease pupae volume and mainly to abnormalities in adult formation, leading to adults dead at hatch. If it is applied low concentration of *B. dracunculifolia* (5–13%) and considering a high concentration of E-nerolidol, an aliphatic sesquiterpene with chemical similarities with JH, in this plant species. We can report an agonist effect on the MET receptor, predicted by the computational protocol, and leading to a larvae prolongation life form period, observed in Larval Toxicity Bioassay (Figs. 6 and 7).

Conclusion And Outlooks

In this study, we propose an *in silico* protocol combining virtual screening, cheminformatics analysis and different metrics of chemical similarity, to predict the most probable targets for typical essential oil (EO) components, as well as the chemical activity relationship orchestrating these actions. Firstly, aiming templates for natural insecticide activity, we have used target models from blowflies, an important livestock pest in Brazil and the world. These same proteins are, however, widespread and conserved along a set of other organisms with agricultural and/or medical importance. Besides that, the same methodology can be extended for a virtually unlimited set of other different targets, transcending the relevance of this work to different potential biotechnological applications.

We established chemical archetypes of “strong insecticide targeting” in EO constituents from this mixed computational approach. Some of these archetypical clusters call attention to the chemical signature significantly like canonical natural insecticides (principally clusters A, B and G; respectively composed of juvenile hormone-like, Steroids-like and substances with organic skeletons close to biogenic amine structures). Besides that, natural compounds with known insecticide activity are found between them, such as E-Nerolidol (Cluster A), reported as an insect repellent, larval biocide, and ovicide.

Trying different similarity metrics from these archetypes for compounds profiled from different EOs, we found that a Euclidean distance-based metric on the cheminformatics space has shown a significant relationship with virtual screening scores using properly calibrated score functions for each target. Using this approach, our protocol could point to different compounds with higher insecticide potential for targets studied here on a set of different EOs. Besides that, the global potential for each EO, as a whole, against each target could be equally estimated based on its chromatographic composition, with an interesting prevalence of signatures for juvenile hormone targeting (MET and JHBP), and octopamine receptor agonism in all the EOs here studied. Experimental bioassays with the EO from leaves of *Baccharis dracunculifolia* against *Chrysomia albiceps* adults and larvae demonstrate mobility, oviposition and anti-metamorphic symptoms consonant with these respective signatures, the same being also corroborated by other literature-reported results. E-nerolidol, in the *B. dracunculifolia* case, seems to be the major compound related to this action. A physiological hypothesis linking the major targets pointed by our computational tool to the symptoms observed on the bioassay is present in Fig. 8.

We hope the computational methodology described here and the results presented in our case studies, will be valuable in shedding a higher light on the nebulous structure-activity relationship between EO composition and their biological actions. We also hope the same methodology can be used in future prospection studies, or even improvement of natural compounds aiming for bioactivity ends. Details of our method calibration and the EO compound database are available in Table S10.

Methods

Molecular target selection and preparation

To understand how essential oils can impact insect metabolism, we surveyed the literature looking for key proteins of insect metabolism: (1) are most often cited as targets of interest and (2) are targeted by current commercial insecticides. After selecting the proteins of interest, we verified the genome of *C. albiceps* to identify the genes corresponding to the same proteins. These sequences were used to search the BLASTp [56] web server for similar proteins with known structures that could be used as templates for comparative modeling of the *C. albiceps'* target proteins 3D conformations. The templates were selected according to their resolution, sequence identity and coverage. We also prioritized sequences from organisms as closely related as possible to the organism of interest and sequences with known agonist and antagonist structures.

For each molecular target, at least three three-dimensional protein models were created using the following software: Chimera [57], Modeller 9.25 [58], Swiss-Model [59], and Phyre2 [60]. Due to limitations of the Phyre2 software when generating agonist and antagonist poses, the EcNR, GABAaR and the OctpR were not modeled using this web-service platform. The final models were selected based on quality criteria provided by each modeling tool and web service quality assessment MolProbity [61], SAVESv6.0 SAVES v6.0 server (https://saves.mbi.ucla.edu/), and PROCHECK [62].

Proteins target models were generated until achieving a model with (1) a low value of RMSD relative to the template; (2) Catalytic or binding amino acid residues were well positioned as described in references; (3) a Low number of outliers and a high percentage of residues in most favorable Ramachandran plot areas; (4) Best indicators quality generated by the respective modeling software. The model's final quality is presented in Tables S2 to S5.

By producing multiple modeling-molecular protein models using different homology-modeling platforms, we can create an experimental design similar to the Randomized Complete Block Design (RCBD), where each model is considered an experimental block, each ligand like a treatment, and each docked pose as a repetition. In further analyses, we will consider the arithmetic mean of the highest docking values and the three highest docking values obtained from docking experiments in each blowfly protein target.

Ligands Dataset preparation

As part of the virtual screening protocol, we performed a series of docking simulations using AutoDock Vina 1.1.2 [21] (Vina) and MGLTools [63] to evaluate how likely the compounds were commonly found in EOs to bind to the selected blowfly targets. The ligand library contains 481 compounds derived from the SISTEMAT eXtended (SistematX) DataBase [64] after filtering out compounds in plant EOs. We also added 170 compounds from gas chromatography of five common plant species of interest to the dataset, totaling 651 ligands. These species of interest are *B. dracunculifolia*, *B. retusa*, *M. urundeuva*, *C. viminalis* and *D. spathulata*.

We eliminated identicalness in the Dataset by calculating the Tanimoto similarity coefficient using the RDKit Python Library [65]. Those with a similarity score of 1.0 were discarded from the Dataset. We created the 3D structure of each remaining compound from their SMILEs using Schrodinger's Lig Prep

[66], considering a pH of 6.4 ± 0.5 and all possible tautomer and stereoisomers. Thus, our final ligand Dataset has 7222 3D-MOL2 structures.

Scoring function selection

To reduce inherent biases in scoring functions, we adopted five scoring functions to evaluate the ligands: Vina [21], Ad4_scoring [22], Dkoes_scoring [22], Vinardo [23] and Convex-PL [24]. The Vina or Autodock Vina score function is an empirical and knowledge-based scoring function based on the X-Score function [21]. Convex-PL is a knowledge-based score function [24]. The last three scoring functions are Smina, a fork of Autodock Vina that can be customized to improve performance using high-performance energy minimization [22]. Ad4_scoring is a semiempirical Autodock 4 AMBER force field function that uses the Coulomb potential, Lennard-Jones potential, desolvation and potential conformational entropy related to the number of rotational bonds [63]. The Dkoes_scoring function is the custom function whose parameter function terms and the methodology to develop it is described by Koes et al. (2013) [22]. Vinardo scoring function has a modified combination of weights parameters to determine atomic radii and a lower number of parameters to describe simplified atomics interactions compared to Vina [23].

For each molecular target, it is determined the score functions which efficiently recover true ligands. We analyzed the behavior of their receiver operating characteristics curves (ROC curve) and the area under the ROC curve (AUC) as well as the enrichment factors curve (EFs curve) calculated by the formula below. It is maximum (EFmax) [25, 26]. Firstly, we identified the true ligands by surveying the literature for bioassays using the target protein expressed in a cell or *in vitro*, considering the agonist or antagonist conformations [25]. Ligands with reported IC_{50}, EC_{50}, K_i, or K_d metrics were selected as true ligands (Table S8) and then generated decoys using the DUD-E web service [67]. The validation set of ligands was submitted to docking simulations using Vina and rescored according to all the additional scoring functions, resulting in five different rankings. Finally, we used these rankings to build the ROC and EF curves for every scoring function presented in Figures S1 to S8.

$EF = \frac{Ntruepositiveatdockingtimelinepoint/Ntotalligandsdockedatdockingtimelinepoint}{Ntotaltruepositivedatabase/Ntotaloficligandsdatabase}$ [26].

Docking score function selection

A good scoring function is expected to rank all the best ligands before the decoys when performing docking simulations. In this ideal situation, the ROC curve would rapidly reach 100% of True positives, resulting in an AUC value of approximately 1, and the EFs curve would peak as soon as the point corresponding to the percentage of the database that corresponds to the good ligands, as shown in the equation below. We established that proper scoring functions would have an AUC value of 0.5 or greater and reach EFMax no later than 5% of the base (1.609 in the log scale shown in Figures S1 to S8). We evaluated these curves in two ways: (1) using the best average score of each ligand across all models for a given molecular target and (2) using the average of the top three scores of each ligand across all models of a target. We then selected the approach that gave the best combination of AUC and EFMax.

At least one score function was chosen for each protein target (highlighted in yellow in Figures S1 to S8). For AChE is selected the mean of the top three scores using the functions Vina, Convex-PL, and Vinardo (AUC = 0.753, 0.798 and 0.708; and EFmax = 24.4057, 24.4057 and 4.0677, respectively). EcNR was evaluated using all score functions (AUC: Vina = 0.475, Convex-PL = 0.636, Ad4_scoring = 0.604, Dkoes_scoring = 0.604, Vinardo = 0.587; EFmax: 25.15, 40.24, 15.1, 15.1 and 37.72, respectively). For JHBP we selected Convex-PL (AUC = 507, EFmax = 3.72) and Vinardo (AUC = 0.888, EFmax = 6.92). For MET, we considered the mean of the top three scores using Convex-PL (AUC = 0.728, EFmax = 6.22) and Ad4_scoring (AUC = 0.862, EFmax = 16.60). GABAaR in agonist and antagonist conformation has used the mean of the top three scores. In agonists we selected Ad4_scoring (AUC = 0.335, EFmax of 3.71) and Dkoes_scoring (AUC = 0.324, EFmax = 1.79). As for the antagonist conformation, the only score function chosen was Vina (AUC = 0.88 and EFmax = 5.61). The OctpR agonist has used the mean of the three highest score values, and the Vina (AUC = 0.565, EFmax = 12.10), Ad4_scoring (AUC = 0.519, EFmax 18.15), Dkoes_scoring (AUC = 0.497, EFmax = 5.18), Vinardo (AUC = 0.629, EFmax = 12.10) functions. In antagonist OctpR, we used only the best average score and the functions Dkoes_scoring (AUC = 0.776, EFmax = 12.40), and Vinardo (AUC = 0.353, EFmax = 34.08).

Docking results post-processing

We adopted a clustering-based consensus approach to consider the scores given by the different functions and determine the high-scored overall natural dataset compounds. For each target, the N-selected scoring functions according to the ROC and EF approaches were used to generate N-dimensional vectors containing the scores given by each function to that ligand as elements. These vectors were used to perform successive k-means clustering, and, in each iteration, the cluster with the best combination of scores was kept. The procedure was repeated until only 8 to 12 unique ligands (not considering enantiomers) were selected for each target.

A final set containing the top ligands of every target was constructed, and after eliminating duplicates, the pairwise Tanimoto distance was calculated. This distance metric was used for hierarchical clustering to establish clusters of chemically similar compounds, the cutoff is determined using the procedure displayed in Figure S11. Each cluster was related to the targets by counting the percentage of the target's top ligands that belonged to it.

A k-means clustering procedure using the centroids and Euclidean distance was applied to allocate the EOs compounds from the five plant species of interest to each cluster. It enables us to compare a wide diversity of natural molecule similarities using different metrics to compare molecular fingerprints [8]. The Tanimoto coefficient is a widely used metric for chemical similarity [8]. In the end, it is possible to validate the degree of influence of each EOs extracted from different plant species in the blowfly protein target.

In other words, the 651 unique natural compounds in the dataset. K-means clustering was applied successively on the results data considering only the best score functions of Enrichment and ROC curves analysis until the 8 to 12 top hits ligands for each blowfly target.

Cheminformatics molecular descriptors were determined using free tools Molinspiration web service [68], ACD/ChemSketch [69] and web service 3D-QSAR.com [70]. The descriptors' values are z-scores to allow the possible comparison among them, doing

$$zScoredMolecularDescriptor = \left(\frac{value - meanofallvaluesforeachdescriptor}{standarddeviationofallvaluesforeachdescriptor} \right)$$

After that, the Cartesian Euclidean distances are calculated for each compound to each cluster defined as mentioned above. A relative normalization and a conversion to the measure of proximity were necessary; therefore, to normalize the values, we divide all Cartesian Euclidean distances by the higher distance obtained, making all Cartesian distances between 1.0 and 0.0:

$$NormalizedEuclideanDistance = \left(\frac{valueofEuclideandistance}{higherEuclideandistance} \right)$$

The measured proximity was calculated by subtracting the Normalized Euclidean Distance from 1. At the final calculations, we obtain a matrix of normalized proximity from the 0.1% hits ligands to each target.

Experimental Blowfly Symptoms caused by Essential oil application

The experimental assays were done using the *C. albiceps* [44], a blowfly frequently observed in the Minas Gerais state, Brazil poultry houses. The blowflies were captured and kept in plastic cages with sawdust on the ground and fed with fresh beef. The EOs used in the experiment were obtained by Hydro-Distillation for 3 hours in Clevenger apparatus using 150 grams of fresh. The yielded EOs are conserved at -5ºC and sheltered from light [71]. Quantitative and qualitative chemical analyses of EOs extracted were performed according to the methodology adopted by Oliveira et al. (2022) [72], with modifications. Chemical constituents were identified by comparing their retention rates against a standard solution co-injection, library databases, and literature [73, 74, 75]. The retention rates were calculated by the equation of Van Den Dool & Kratz (1963), and the retention rates described in the literature were consulted [73, 74, 75, 76].

Fumigant Activity Bioassay Five days-old blowflies' adults were used on a Fumigant Toxicity bioassay. Ten adults were placed inside Erlenmeyer glasses and closed; a 10 cm cotton string, previously soaked with a 1ml treatment solution ranging from 0 to 30% of *B. dracunculifolia* Essential oil, immersed in the solution for one minute, was fixed in the middle of Erlenmeyer's lid [77]. Mortality (%) and qualitatively abnormal behavior were registered at one hour, three hours, 22h and 24h. Each treatment was repeated three times.

Larval Toxicity Bioassay Larvae showing site-seeking behavior for pupation were used immediately in larval toxicity bioassays. Twenty larvae were treated with an EO serial dilution ranging from 0–30%, following the protocol established by Chaaban et al. (2018) [40]. Survivors' number, morphological and

behavior change, pupae dimensions, and adult morphological aspects were evaluated every 12 hours until the adult emergence. Ten-second videos of the larvae were recorded using Samsung Galaxy A30s at forty-eight hours after the treatment. These videos were stabilized and standardized to 60 frames per second using DaVinci Resolve [78] software. A custom python script using the OpenCV 4.5.4 library [79] was created to measure the average larval motility by 1. Creating a black and white image, where white pixels corresponded to the larvae and had a value of 1 while background pixels were black with a value of 0; 2. Flattening the matrix corresponding to the frame to obtain a vector; 3. Measuring the cosine distance between each frame and its predecessor; 4. Averaging the measured distances. The cosine distance of two vectors equals one minus the cosine of the angle between them. It is a more suitable proxy for the larval motility than the Euclidean distance because it is indifferent to the length of the vector (which is proportional to the number of white pixels in the image), which translates into a more reliable comparison between videos in which larvae sizes (thus the number of white pixels) might vary.

Declarations

Data availability statement (mandatory)

The data to reproduce the experiments performed here as well as the scripts used are available the following GitHub repository: https://github.com/fccarvalho2/Essential_oil_Screening.git

Acknowledgments

We are grateful to Coordination for the Improvement of Higher Education Personnel (CAPES), Minas Gerais Research Funding Foundation (FAPEMIG) and the National Council for Scientific and Technological Development (CNPq) for financial support of this research. Professor Luciana Alves Rodrigues dos Santos Lima (UFSJ), Dr Mairon César Coimbra (UFSJ), Ricardo Nascimento Araujo (UFMG). In memory of Professor Stênio Nunes Alves deceased by Covid-19.

Author Contributions Statement

All authors contributed substantially to the reported work. E.J.A.C.: Performed experimental and computational experiments and wrote the research manuscript; F.C.C.: Coordinated the in silico experimental; J.A.D.C.O. and S.K.V.B.: Performed the Gas Chromatography Profiles of *Baccharis dracunculifolia*, *Baccharis retusa* and *Disynaphia spathulata*; C.H.S.: Collaborated during the virtual screening analysis; F.C.G.: Oriented the virtual screening; M.T.S.: Was responsible for and curating the SistematX natural ligands database used in this research, he helps us to find the plant natural ligands in the natural database; J.O.F.M.: Performed the Gas Chromatography Profiles of *Myracrodruon urundeuva* and *Callistemon viminalis*; R.C.M.M.: Coordinated the computational section of this research, and L.H.F.L.: Coordinate the research work. All authors reviewed the manuscript.

Additional Information

Supplementary information accompanies this paper.

Competing interests' statement: The authors declare no competing interests.

SISBio registration for collecting botanical, fungal and microbiological material: Number 64608.

References

1. Elshafie HS, Camele I. An Overview of the Biological Effects of Some Mediterranean Essential Oils on Human Health. Biomed Res Int. 2017 2017: 9268468. doi: https://doi.org/10.1155/2017/9268468
2. Ootani MA, Aguiar RW, Ramos ACC, Brito DR, da Silva JB, Cajazeira JP. Use of Essential Oils in Agriculture. Journal of Biotechnology and Biodiversity 2013 4(2): 162-174, May 2013 ISSN: 2179-4804
3. Mladenović M, Arsić BB, Stanković N, Mihović N, Ragno R, Regan A, Milićević JS, Trtić-Petrović TM, Micić R. The Targeted Pesticides as Acetylcholinesterase Inhibitors: Comprehensive Cross-Organism Molecular Modelling Studies Performed to Anticipate the Pharmacology of Harmfulness to Humans *In Vitro*. Molecules 2018 23(9): 2192. doi: https://doi.org/10.3390/molecules23092192
4. Jankowska M., Rogalska J., Wyszkowska J., Stankiewicz M., 2018. Molecular targets for components of essential oils in the insect nervous system—a review. Molecules 2018 23(1). doi: https://doi.org/10.3390/molecules23010034
5. Charles JP, Iwema T, Epa VC, Takaki K, Rynes J, Jindra M. Ligand-binding properties of a juvenile hormone receptor, Methoprene-tolerant. Proc Natl Acad Sci USA 2011 108(52): 21128-33. doi: https://doi.org/10.1073/pnas.1116123109
6. Smagghe G. Ecdysone, structures and functions. 1st ed. Dordrecht:Springer; 2009. doi: https://doi.org/10.1007/978-1-4020-9112-4
7. Kim IH, Pham V, Jablonka W, Goodman WG, Ribeiro JMC, Andersen JF. A mosquito hemolymph odorant-binding protein family member specifically binds juvenile hormone. J Biol Chem. 2017 15;292(37): 15329-15339. doi: https://doi.org/10.1074/jbc.M117.802009
8. Santana K, do Nascimento LD, Lima e Lima A, Damasceno V, Nahum C, Braga RC and Lameira J (2021) Applications of Virtual Screening in Bioprospecting: Facts, Shifts, and Perspectives to Explore the Chemo-Structural Diversity of Natural Products. Front. Chem. 9:662688. doi: https://doi.org/10.3389/fchem.2021.662688
9. Chen Y, Kirchmair J. Cheminformatics in Natural Product-based Drug Discovery. Mol Inform. 2020 Dec;39(12):e2000171. doi: https://doi.org/10.1002/minf.202000171
10. Lin, E.; Lin, C.-H.; Lane, H.-Y. Relevant Applications of Generative Adversarial Networks in Drug Design and Discovery: Molecular De Novo Design, Dimensionality Reduction, and De Novo Peptide and Protein Design. Molecules 2020, 25, 3250. doi: https://doi.org/10.3390/molecules25143250
11. Grisi L, Leite RC, Martins JRDS, Barros ATMD, Andreotti R, Cançado PHD, León AAP, Villela HS. Reassessment of the potential economic impact of cattle parasites in Brazil. Revista Brasileira de Parasitologia Veterinária 2014 23(2): 150-156. doi: https://doi.org/10.1590/s1984-29612014042

12. Ishaaya I. Biochemical Sites of Insecticide Action and Resistance. 1st ed. Heidelberg: Springer; 2001. doi: https://doi.org/10.1007/978-3-642-59549-3
13. Nation Sr. JL. Insect Physiology and Biochemistry. 3rd ed. Boca Raton: CRC Press; 2015. doi: https://doi.org/10.1201/9780429277658
14. Correa EJA, Alves SN, Coimbra MC, Lima LHF. The potential of the genus Baccharis spp. as an insecticide for mosquitoes and non-biting flies of veterinary importance. In: Singh HB, Vaishnav A, editors. New and Future N Developments in Microbial Biotechnology and Bioengineering Sustainable Agriculture: Revitalization Through Organic Products. Amsterdam:Elsevier; 2022. p. 111-129. doi: https://doi.org/10.1016/B978-0-323-85579-2.00012-5
15. Roeder T. Octopamine in invertebrates. Prog Neurobiol. 1999 59(5): 533-561. doi: https://doi.org/10.1016/s0301-0082(99)00016-7
16. Ormerod KG, Hadden JK, Deady LD, Mercier AJ, Krans JL. Action of octopamine and tyramine on muscles of Drosophila melanogaster larvae. J Neurophysiol. 2013 Oct;110(8):1984-96. doi: https://doi.org/10.1152/jn.00431.2013
17. Li F, Li K, Wu L-J, Fan Y-L, Liu T-X. Role of Biogenic Amines in Oviposition by the Diamondback Moth, Plutella xylostella L. Front. Physiol. 2020 11:475. doi: https://doi.org/10.3389/fphys.2020.00475
18. Thompson CS, Yagi KJ, Chen ZF, Tobe SS. The effects of octopamine on juvenile hormone biosynthesis, electrophysiology, and cAMP content of the corpora allata of the cockroach *Diploptera punctata*. J Comp Physiol B. 1990 160(3): 241-9. doi: https://doi.org/10.1007/BF00302589
19. Fahrbach SE, Smagghe G, Velarde RA. Insect Nuclear Receptors. Annual Review of Entomology 2012 57: 83-106. doi: https://doi.org/10.1146/annurev-ento-120710-100607
20. Kim IH, Castillo JC, Aryan A, Martin-Martin I, Nouzova M, Noriega FG, Barletta ABF, Calvo E, Adelman ZN, Ribeiro JMC, Andersen JF. A mosquito juvenile hormone binding protein (mJHBP) regulates the activation of innate immune defenses and hemocyte development. PLOS Pathogens 2020 16(1): e1008288. doi: https://doi.org/10.1371/journal.ppat.1008288
21. Trott O, Olson AJ (2009). AutoDock Vina: Improving the speed and accuracy of docking with a new scoring function, efficient optimization, and multithreading. Journal of Computational Chemistry 2009 31(2): 455–461. doi: https://doi.org/10.1002/jcc.21334
22. Koes DR, Baumgartner MP, Camacho CJ. Lessons learned in empirical scoring with smina from the CSAR 2011 benchmarking exercise. J Chem Inf Model. 2013 53(8): 1893-904. doi: https://doi.org/10.1021/ci300604z
23. Quiroga R, Villarreal MA. Vinardo: A Scoring Function Based on Autodock Vina Improves Scoring, Docking, and Virtual Screening. PLOS ONE 2016 11(5): e0155183. doi: https://doi.org/10.1371/journal.pone.0155183
24. Kadukova M, Grudinin S. Convex-PL: a novel knowledge-based potential for protein-ligand interactions deduced from structural databases using convex optimization. J Comput Aided Mol Des. 2017 31(10): 943-958. doi: https://doi.org/10.1007/s10822-017-0068-8

25. Rocha REO. Prospecção de Inibidores Ortostéricos da protease NS2B-NS3 do vírus zika como potenciais candidatos a fármacos. [Thesis work] Federal University of Minas Gerais State. 58p. Forthcoming 2017.
26. Huang N, Shoichet BK, Irwin JJ. Benchmarking sets for molecular docking. J Med Chem. 2006 Nov 16;49(23):6789-801. doi: https://doi.org/10.1021/jm0608356
27. Antonio G.Gonzalez AG, Jimenez IA, Ravelo AG, Coll J, Gonzalez JA, Lloria J. Antifeedant Activity of Sesquiterpenes from Celastraceae. Biochemical Systematics and Ecology 1997 25(6): 513-519. doi: https://doi.org/10.1016/S0305-1978(97)00035-5
28. Chan WK, Tan LT, Chan KG, Lee LH, Goh BH. Nerolidol: A Sesquiterpene Alcohol with Multi-Faceted Pharmacological and Biological Activities. Molecules. 2016 Apr 28;21(5):529. doi: https://doi.org/10.3390/molecules21050529
29. Ghoneim K, Hamadah Kh., Selim Sh, Waheeb H. Biopesticidal Potential of Nerolidol, a Sesquiterpene Compound, and its Drastic Impact on Growth and Metamorphosis of the Cotton Leafworm Spodoptera littoralis (Lepidoptera: Noctuidae). Scholars Academic Journal of Biosciences 2021 9(2): 36-57. doi: https://doi.org/10.36347/sajb.2021.v09i02.004
30. Juan Hikawczuk VE, Saad JR, Giordano OS, García C, Martín T, Martín VS, Sosa ME, Tonn CE. Insect growth regulatory effects of linear diterpenoids and derivatives from Baccharis thymifolia. J Nat Prod. 2008 Feb;71(2):190-4.doi: https://doi.org/10.1021/np070392o
31. Wu HB, Wu HB, Wang WS, Liu TT, Qi, MG, Feng JC, Li ZY, Liu Y. Insecticidal activity of sesquiterpene lactones and monoterpenoid from the fruits of Carpesium abrotanoides. Industrial Crops and Products 2016 92. 77-83. doi: https://doi.org/10.1016/j.indcrop.2016.07.046
32. Elufioye TO, Obuotor EM, Agbedahunsi JM, Adesanyad SA. Cholinesterase inhibitory activity and structure elucidation of a new phytol derivative and a new cinnamic acid ester from *Pycnanthus angolensis*. Revista Brasileira de Farmacognosia 2016 26(4): 433-437. doi: https://doi.org/10.1016/j.bjp.2016.01.010
33. Van Wyk HM, Schoeman D, Kwembeya E, Hans RH, Pool EJ, Louw S. *In vitro* acetylcholinesterase inhibitory activity and chemical composition of the dichloromethane extracts of the leaves and inflorescences of the tumbleweed, *Trachyandra laxa* (N.E.Br.) Oberm. Var. rigida (Suesseng.) Roessl 2022 South African Journal of Botany 147: 231-237. doi: https://doi.org/10.1016/j.sajb.2021.12.013
34. Eldeen IMS, Hamid A, Wong KC, Abdullah MA, Tengku-Muhammad TS, Abdillahi HS, Van Staden J. *In vitro* repression of cyclooxygenase, acetylcholinesterase activities and bacterial growth by trans-phytol and a glycolipid from the leaves of *Homalomena sagittifolia* 2016 Res. J. Med. Plants 10: 320-329. doi: https://doi.org/10.3923/rjmp.2016.320.329
35. Elufioye TO, Obuotor EM, Agbedahunsi JM, Adesanya SA. Anticholinesterase constituents from the leaves of Spondias mombin L. (Anacardiaceae). Biologics. 2017 Aug 2;11:107-114. doi: https://doi.org/10.2147/BTT.S136011
36. Tchekalarova J, Freitas RM. Effect of Diterpene Phytol on Pentylenetetrazol and Maximal Electroshock Seizure Models: Possible Role of GABAergic Mechanism. Pharmacologia 2014 5(9):

351-356. doi: https://doi.org/10.5567/pharmacologia.2014.351.356

37. Costa JP, de Oliveira GA, de Almeida AA, Islam MT, de Sousa DP, de Freitas RM. Anxiolytic-like effects of phytol: possible involvement of GABAergic transmission. Brain Res. 2014 Feb 14;1547:34-42. doi: https://doi.org/10.1016/j.brainres.2013
38. Şengül Demirak MŞ, Canpolat E. Plant-Based Bioinsecticides for Mosquito Control: Impact on Insecticide Resistance and Disease Transmission 2022 Insects 2022 13(2):162. doi: https://doi.org/10.3390/insects13020162
39. Khyade VB, Shinde VD, Maske SS. Influence of the diterpenoids (Retinol and Phytol) (Race: PM x CSR2) on the cocoon and silk parameters in silkworm, Bombyx mori (L) (Race: PM x CSR2) 2016 World Scientific News 42:1-12.
40. Lobato JN, Azevedo RS, Correa EJA, Parreira AG, Alves SN, Silva AF. Cerrado Brazilian Biome: Characterization and Importance. International Invention of Scientific Journal 2017 1: 1-19.
41. Figueiredo YG, Corrêa EA, de Oliveira Junior AH, Mazzinghy ACDC, Mendonça HDOP, Lobo YJG, García YM, Gouvêia MADS, de Paula ACCFF, Augusti R, Reina LDCB, da Silveira CH, de Lima LHF, Melo JOF. Profile of Myracrodruon urundeuva Volatile Compounds Ease of Extraction and Biodegradability and In Silico Evaluation of Their Interactions with COX-1 and iNOS. Molecules. 2022 Mar 1;27(5):1633. doi: https://doi.org/10.3390/molecules27051633
42. Silva CJ, Oliveira Junior, AH, Mendonça HO, Correa EJA, Gouveia MAS, Figueiredo YG, Paula ACCFF, Lima LHF Augusti R, Melo JOF. Chapter 7 - Water Stress-Induced Changes in the Physiology of Callistemon viminalis, Essential Oil Composition and Predicted Biological Activity. In: Zhanibek Yessimbekov. (Org.). Advances in Agricultural and Life Sciences. 1ed.Zittau, Germany: Weser Books, 2021, v. 5, p. 125-149.
43. Ahern JR, Whitney KD. Sesquiterpene lactone stereochemistry influences herbivore resistance and plant fitness in the field. Ann Bot. 2014 Mar;113(4):731-40. doi: https://doi.org/10.1093/aob/mct297
44. De Carvalho C and Ribeiro P. Chave de identificação das espécies de Calliphoridae (Diptera) do Sul do Brasil. Brazilian journal of veterinary parasitology 2000 9:169-173.
45. Chaaban A, Martins CEN, Bretanha LC, Micke GA, Carrer AR, Rosa NF, Ferreira L, Moleto, MB. Insecticide activity of Baccharis dracunculifolia essential oil against Cochliomyia macellaria (Diptera: Calliphoridae). Natural Product Research 2018 32(24): 2954-2958, doi: https://doi.org/10.1080/14786419.2017.1392947
46. Kammer, A.E., Rheuben, M.B. (1981). Neuromuscular Mechanisms of Insect Flight. In: Herreid, C.F., Fourtner, C.R. (eds) Locomotion and Energetics in Arthropods. Springer, Boston, MA. doi: https://doi.org/10.1007/978-1-4684-4064-5_7
47. Schendzielorz T, Schirmer K, Stolte P, Stengl M. Octopamine regulates antennal sensory neurons via daytime-dependent changes in cAMP and IP3 levels in the hawkmoth Manduca sexta. PLoS One. 2015 10(3): e0121230. doi: https://doi.org/10.1371/journal.pone.0121230
48. Rien D, Kern R and Kurtz R. Octopaminergic modulation of a fly visual motion-sensitive neuron during stimulation with naturalistic optic flow 2013 Frontiers in Behavioral Neuroscience 7: 1-14. doi:

https://doi.org/10.3389/fnbeh.2013.0015

49. O'Gara BA and Drewes CD. Modulation of tension production by octopamine in the metathoracic dorsal longitudinal muscle of the cricket Teleogryllus oceanicus. J Exp Biol 1 1990 149(1): 161–176. doi: https://doi.org/10.1242/jeb.149.1.161
50. Thompson CS, Tobe SS. Chapter Innervation and Electrophysiology of the Corpus Allatum. In: Huber B, Master EP, Rao BR, Cockroaches as Models for Neurobiology: Applications in Biomedical Research. 1st Edition. Boca Raton:CRCPress; 1990. doi: https://doi.org/10.1201/9781351070751
51. Wigglesworth, V. The Corpus Allatum and the Control of Metamorphosis in Insects. Nature 1947 159: 872. doi: https://doi.org/10.1038/159872a0
52. Zhang X, Li S and Liu S. Juvenile Hormone Studies in Drosophila melanogaster. Front. Physiol. 2022 12:785320. doi: https://doi.org/10.3389/fphys.2021.785320
53. King JE, Bennett GW, Mortality and Developmental Abnormalities Induced by Two Juvenile Hormone Analogs on Nymphal German Cockroaches (Dictyoptera: Blattellidae), Journal of Economic Entomology 1988 81(1): 225–227. doi: https://doi.org/10.1093/jee/81.1.225
54. Khater H. Bioactivity of essential oils as green biopesticides: Recent global scenario, January 2013. In: Govil JN, Bhattacharya, S. Recent Progress in Medicinal Plants, Vol. 37; Essentials Oils II Houston:Studium Press LLC; 2013. pp.151-218
55. Rolff J, Johnston PR, Reynolds S. Complete metamorphosis of insects. Phil. Trans. R. Soc. B 2019 374: 20190063.doi: http://dx.doi.org/10.1098/rstb.2019.0063
56. Altschul SF, Gish W, Miller W, Myers EW, Lipman DJ. Basic local alignment search tool. J Mol Biol. 1990 215(3): 403-10. doi: https://doi.org/10.1016/S0022-2836(05)80360-2
57. Yang Z, Lasker K, Schneidman-Duhovny D, Webb B, Huang CC, Pettersen EF, Goddard TD, Meng EC, Sali A, Ferrin TE. UCSF Chimera, MODELLER, and IMP: an integrated modeling system. J Struct Biol. 2012 179(3): 269-78. doi: https://doi.org/10.1016/j.jsb.2011.09.006
58. Webb B, Sali A. Comparative Protein Structure Modeling Using MODELLER. Curr Protoc Bioinformatics. 2016 54:5.6.1-5.6.37. doi: https://doi.org/10.1002/cpbi.3
59. Waterhouse A, Bertoni M, Bienert S, Studer G, Tauriello G, Gumienny R, Heer FT, de Beer TAP, Rempfer C, Bordoli L, Lepore R, Schwede T. SWISS-MODEL: homology modelling of protein structures and complexes. Nucleic Acids Res. 2018 46: W296-W303. doi: https://doi.org/10.1093/nar/gky427
60. Kelley LA, Mezulis S, Yates CM, Wass MN, Sternberg MJ. The Phyre2 web portal for protein modeling, prediction and analysis. Nature protocols 2015 10(6): 845–858. https://doi.org/10.1038/nprot.2015.053.
61. Williams CJ, Headd JJ, Moriarty NW, Prisant MG, Videau LL, Deis LN, Verma V, Keedy DA, Hintze BJ, Chen VB, Jain S, Lewis SM, Arendall WB 3rd, Snoeyink J, Adams PD, Lovell SC, Richardson JS, Richardson DC. MolProbity: More and better reference data for improved all-atom structure validation. Protein Sci. 2018 Jan;27(1):293-315. doi: https://doi.org/10.1002/pro.3330
62. Laskowski RA, MacArthur MW, Moss DS, Thornton JM. PROCHECK: a program to check the stereochemical quality of protein structures. Journal of Applied Crystallography 1993 26: 283-291.

doi: https://doi.org/10.1107/S0021889892009944

63. Morris GM, Huey R, Lindstrom W, Sanner MF, Belew RK, Goodsell DS, Olson AJ. AutoDock4 and AutoDockTools4: Automated docking with selective receptor flexibility. J Comput Chem. 2009 30(16): 2785-91. doi: https://doi.org/10.1002/jcc.21256
64. Costa RPO, Lucena LF, Silva LMA, Zocolo GJ, Herrera-Acevedo C, Scotti L, Da-Costa FB, Ionov N, Poroikov V, Muratov EN, Scotti MT. The SistematX Web Portal of Natural Products: An Update. J Chem Inf Model. 2021 61(6): 2516-2522. doi: https://doi.org/10.1021/acs.jcim.1c00083
65. RDKit: Open-Source Cheminformatics Software (RRID:SCR_014274)
66. Schrödinger Release 2021-4: LigPrep, Schrödinger, LLC, New York, NY, 2021.
67. Mysinger MM, Carchia M, Irwin JJ, Shoichet BK. Directory of useful decoys, enhanced (DUD-E): better ligands and decoys for better benchmarking. Journal of medicinal chemistry 2017 55(14): 6582–6594. doi: https://doi.org/10.1021/jm3006
68. Mweene P, Muzaza G. Implementation of Interactive Learning Media on Chemical Materials. J. Educ. Verkenn. 2020 1: 8–13.doi: https://doi.org/10.48173/jev.v1i1.24
69. Marpaung DN, Pongkendek JJ, Azzajjad MF, Sukirno S. Analysis of Student Motivation using Chemsketch on Hydrocarbon Topic in SMA Negeri 2 Merauke. J. Appl. Sci. Eng. Technol. Educ. 2021 3: 69–73.doi: https://doi.org/10.35877/454RI.asci105
70. Ragno R. www.3d-qsar.com: A web portal that brings 3-D QSAR to all electronic devices—The Py-CoMFA web application as tool to build models from pre-aligned datasets. J. Comput. Mol. Des. 2019 33: 855–864.doi: https://doi.org/10.1007/s10822-019-00231-x
71. Valter JL, Alencar KMC, Sartori ALB, Nascimento EA, Chang R, Morais SAL, Laura VA, Yoshida NC, Carollo CA, da Silva DB, Grassi RF, Fabri JR Siqueira JM. Chemical variability of the essential oil of the leaves from six individuals of *Duguetia furfuracea* (Annonaceae). Brazilian Journal of Pharmacognosy 2008 18(3): 373-378. doi: https://doi.org/10.1590/S0102-695X2008000300011
72. de Castro Oliveira, J.A., Ferreira, L.S., Garcia, I.P. et al. Eugenia uniflora, Melaleuca armillaris, and Schinus molle essential oils to manage larvae of the filarial vector Culex quinquefasciatus (Diptera: Culicidae). Environ Sci Pollut Res 29, 34749–34758 (2022). doi: https://doi.org/10.1007/s11356-021-18024-x
73. National Institute of Standards and Technology. PC version 2.0 of the NIST/EPA/NIH Mass Spectral Library. Gaithersburg, 2008.
74. Adams RP. Identification of essential oil components by gas chromatography/mass spectrometry. 4.1 ed. Illinois:Allured Publishing; 2017.
75. Tkachev AV. The study of volatile substances of plants. Novosibirsk: Offset; 2008.
76. Van Den Dool H, Kratz PDA. Generalization of the retention index system including linear temperature programmed gas-liquid partition chromatography. Journal of Chromatography 1963 11: 463-471.
77. Fu JT, Tang L, Li WS, Wang K, Cheng DM, Zhang ZX, Fumigant Toxicity and Repellence Activity of Camphor Essential Oil from Cinnamonum camphora Siebold Against Solenopsis invicta Workers

(Hymenoptera:Formicidae). Journal of Insect Science 2015 15(1): 129. doi: https://doi.org/10.1093/jisesa/iev112

78. Blackmagic Design Pty.Ltd. 2022 (version 18). [DaVinci Resolve 18]. [Accessed 12 May 2022].
79. Bradski G (2000). The OpenCV Library. Dr. Dobb's Journal of Software Tools.

Figures

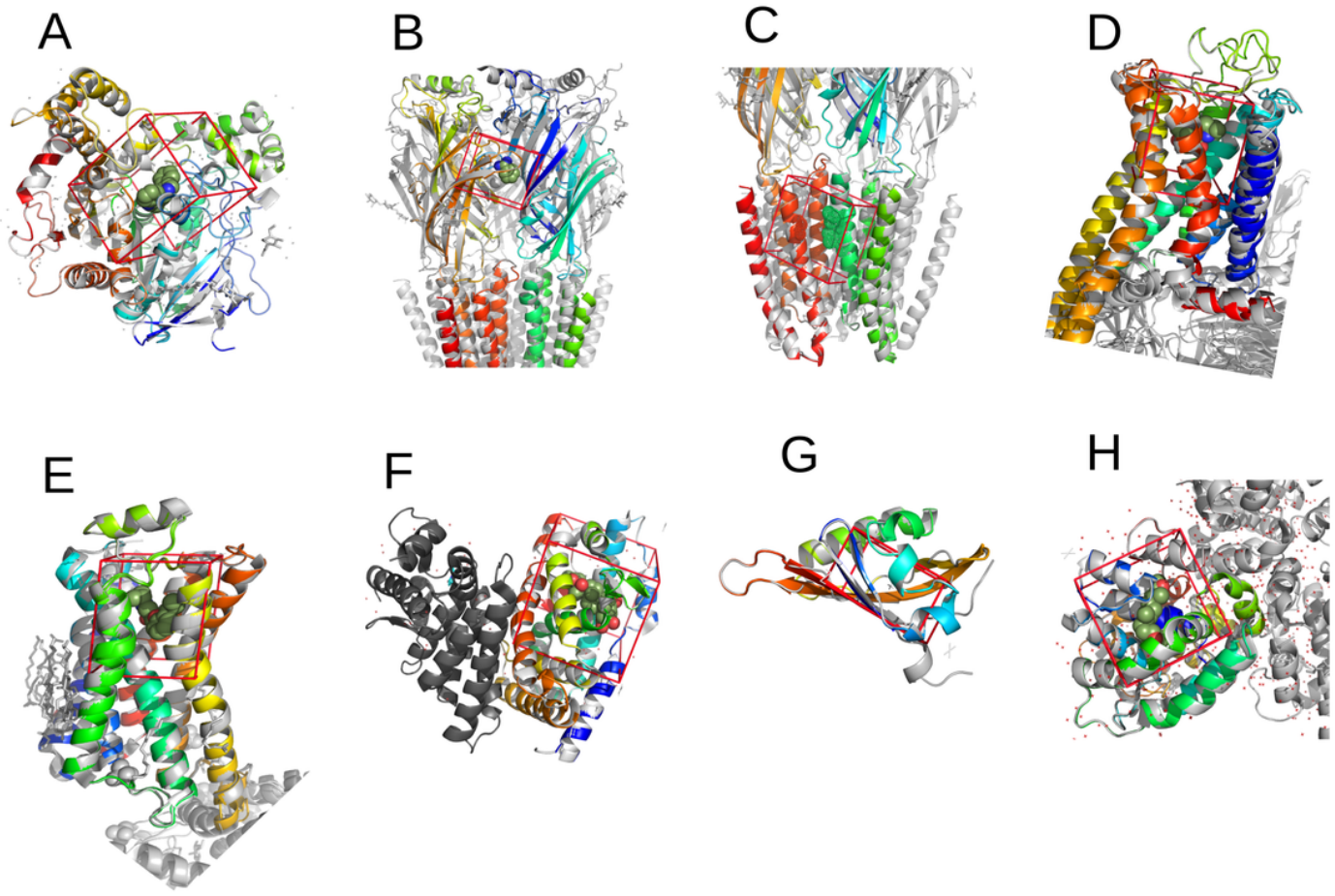

Figure 1

Protein blowfly targets modeled. A-Acetylcholinesterase enzyme; B-γ-Aminobutyric Acid class a receptor agonist; C-γ-Aminobutyric Acid class a receptor antagonist; D-Octopamine receptor agonist; E-Octopamine receptor antagonist; F-Ecdysone Nuclear Receptor; G-Methoprene-Tolerant Juvenile Hormone Receptor; H-Hormone Carrier (Juvenile Odorant family Hormone binding Protein).

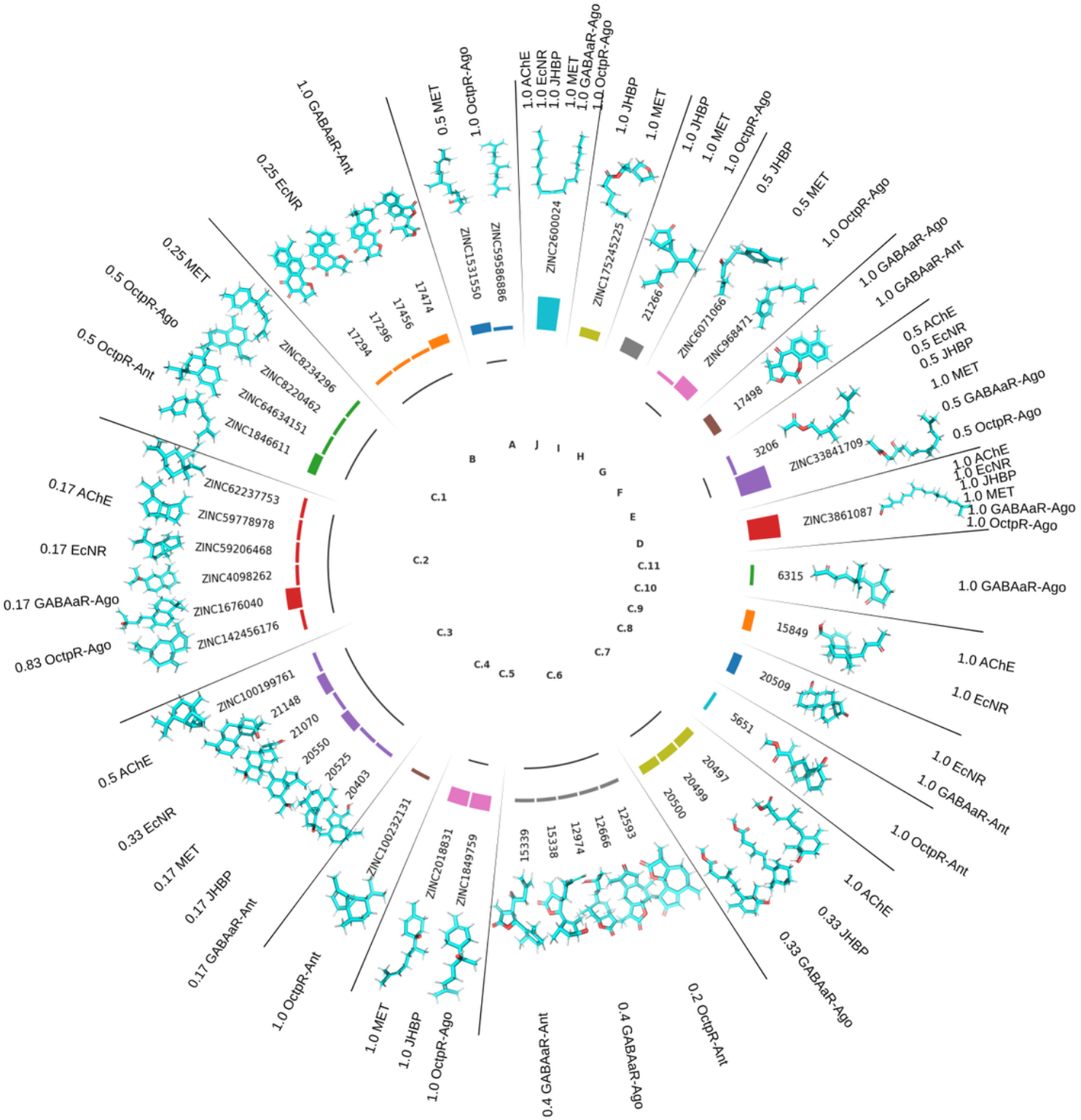

Figure 2

Distribution of hits ligands for blowfly targets among hierarchical clusters, the bar height represents the number of targets high scored by the ligand. The chemical structure is shown, and numbers represent the probability of a blowfly target being affected by the hierarchical cluster.

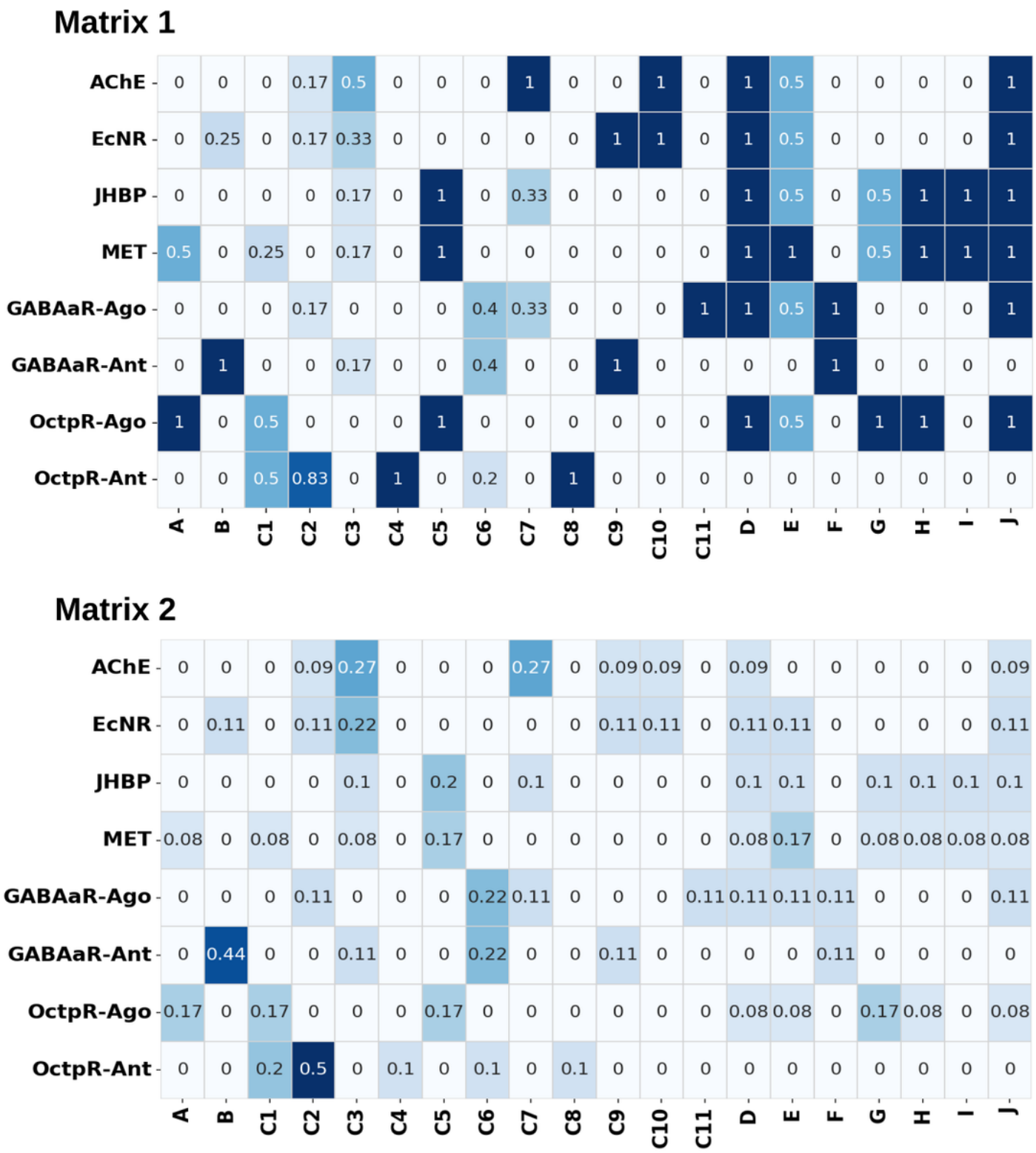

Figure 3

Matrix 1 shows the fraction of hits of ligands belonging to the cluster with high docking scores for the protein target; Matrix 2 otherwise presents the fraction of ligands that affect the protein target which belongs to each cluster.

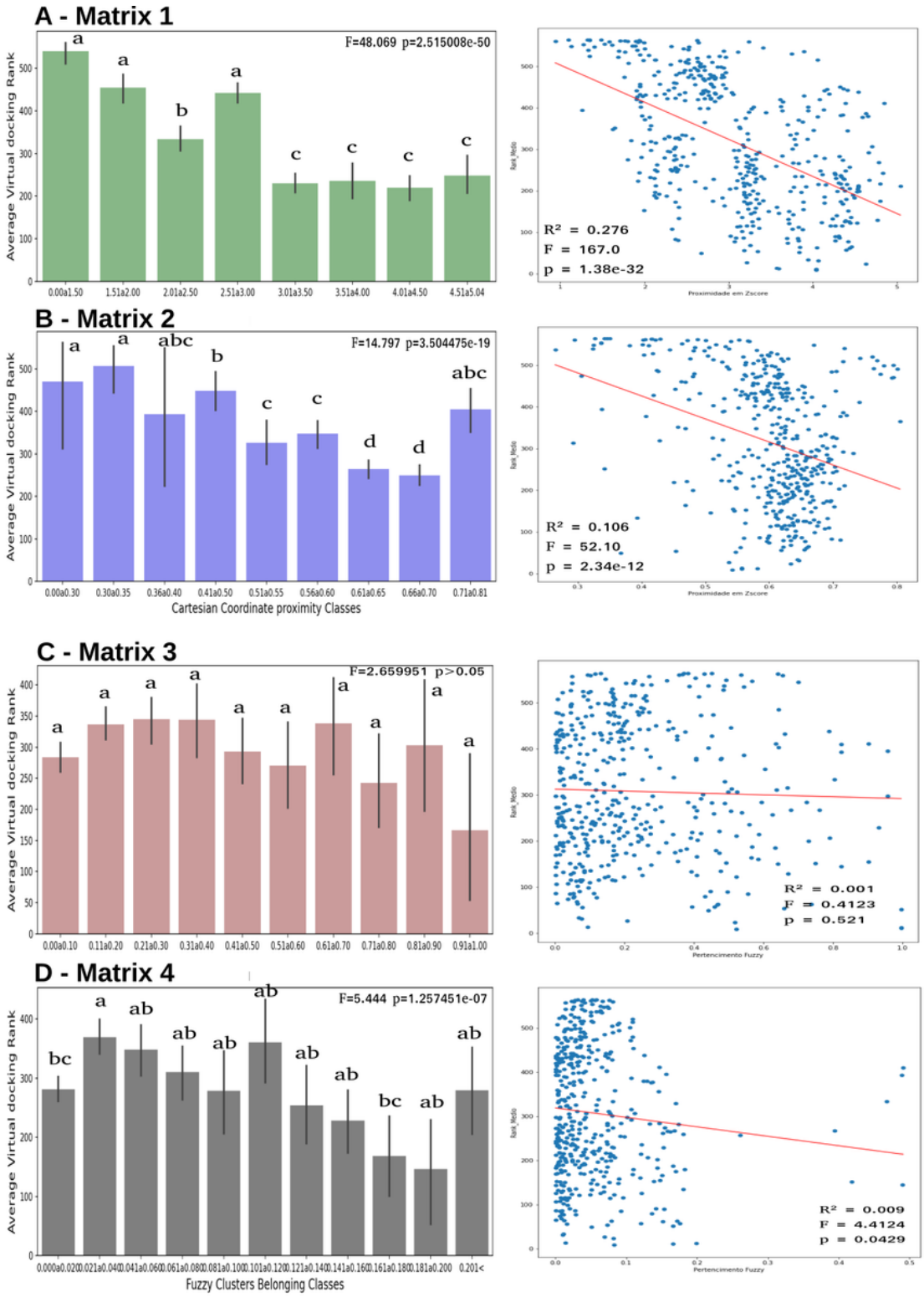

Figure 4

A-Correlation between average docking score rank and Matrix 1: Matrix one multiplied matrix EPNMCS; B-Matrix 2: Matrix two multiplied matrix EPNMCS; C-Matrix 3: Matrix one multiplied matrix BDSTFL; D-Matrix 4: Matrix two multiplied matrix BDSTFL.

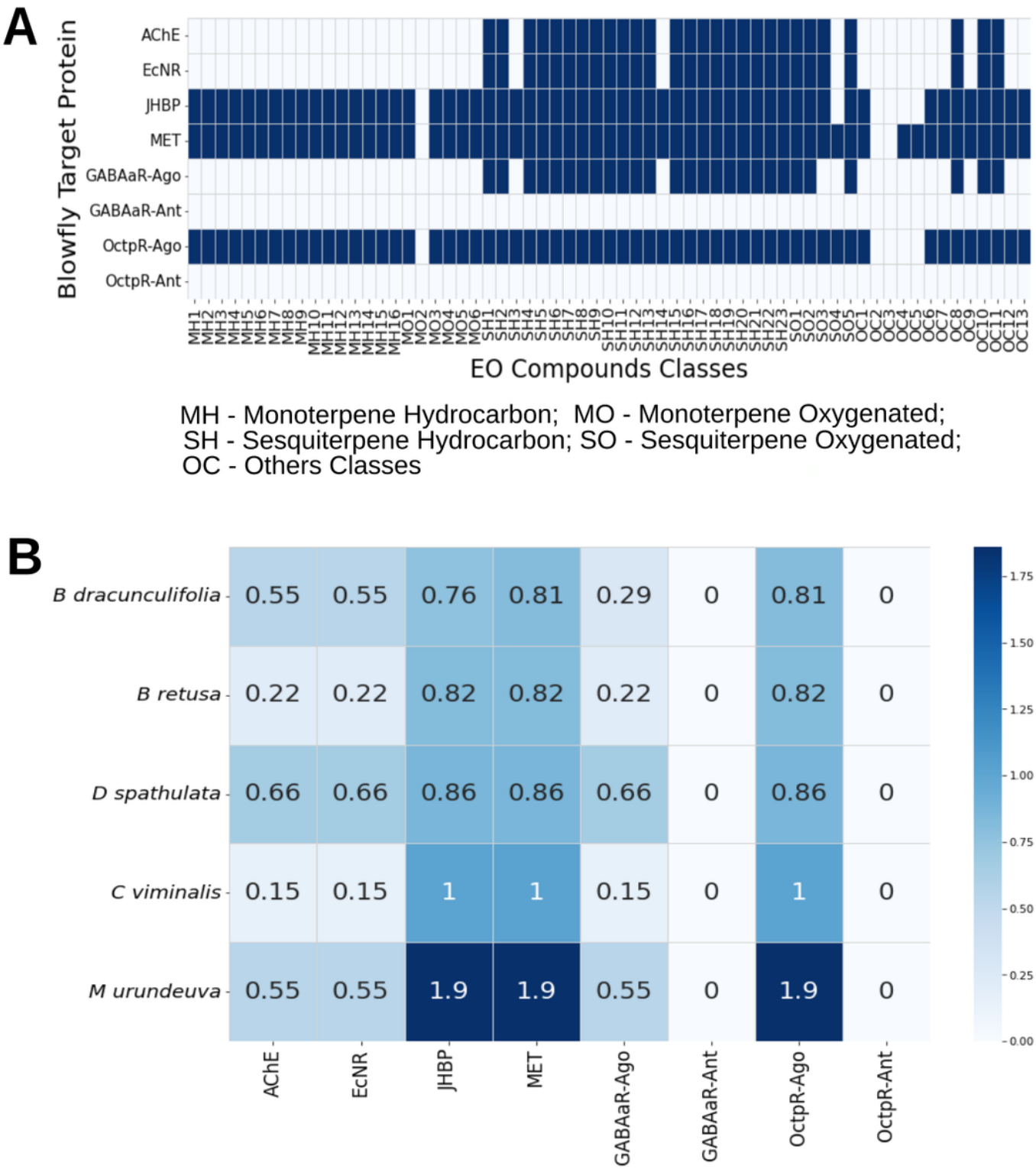

Figure 5

Matrices of likeliness of plant essential oils compounds affect the blowfly's protein target low pale-blue and or high deep blue. ID Numbers refer to EO compounds in the Chemical Chromatographic Profile of plant species shown in Table S6 and published studies [41, 42].

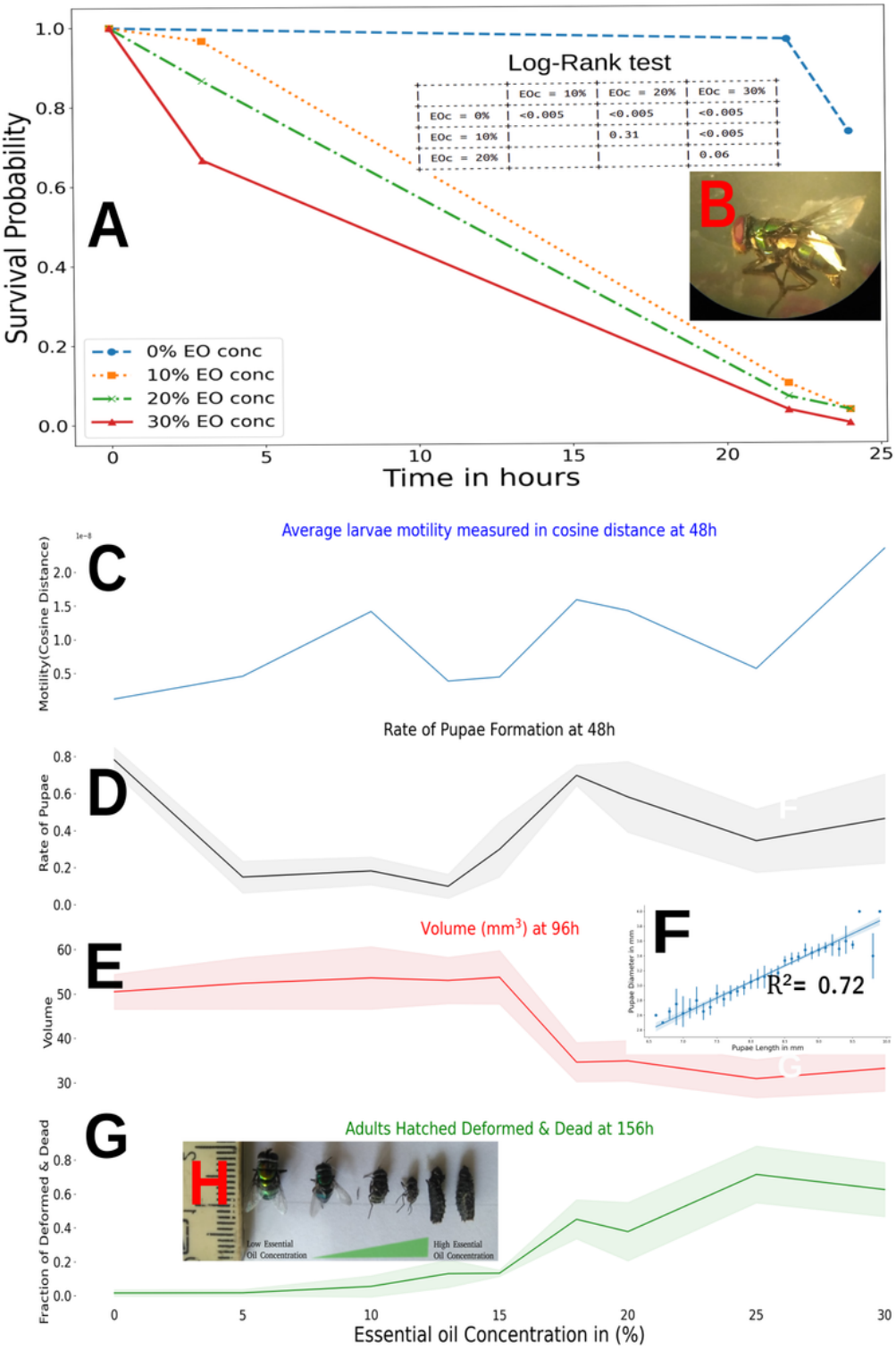

Figure 6

Fumigant Activity Bioassay showing: A-Kaplan–Meier Survival curves and probability Log-Rank test; B-Oviposition by Blowflies submitted EO after 22 hours of bioassay; C-Larval Motility measured in Cosine distance over different EO concentration applied; D-Pupae rate formation after 48h after bioassay start; E-Pupae volume at 96h bioassay; F-Regression among pupae length and diameter; G-Fraction of adults hatched deformed and dead at 156h of bioassay; H-Deformed Adults hatched.

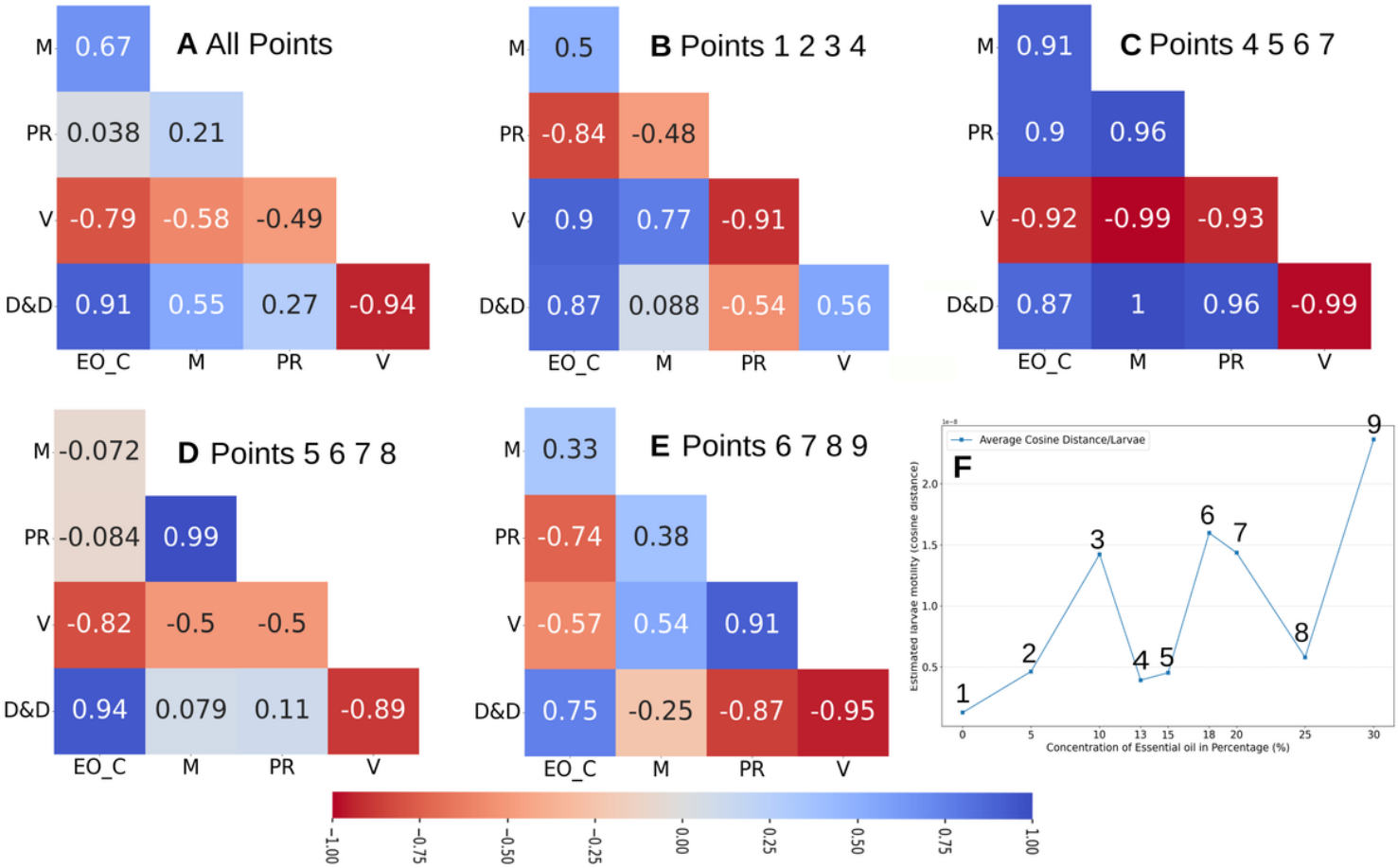

EO_C - Essential oil concentration in %; **M** - Larvae motility estimated in average of cosine distance divided per larvae number; **PR** - Rate of Pupae Formation at 48h; **V** - Pupae Volume in mm3 at 96h; **D&D** - Rate of adults blowflies hatched dead and deformed at 156h.

Figure 7

Correlations among larvae motility, rate of pupae formation, pupae volume (mm^3), and the fraction of adult flies hatched deformed and dead considering the points among: A-EO concentrations 0 to 30%; B-EO concentrations 0 to 13%; C-EO concentrations 13 to 20%; D-EO concentrations 15 to 25%; E-EO concentrations 18 to 30%; F-Numbering points of Larvae motility curve to be correlated with bioassay data.

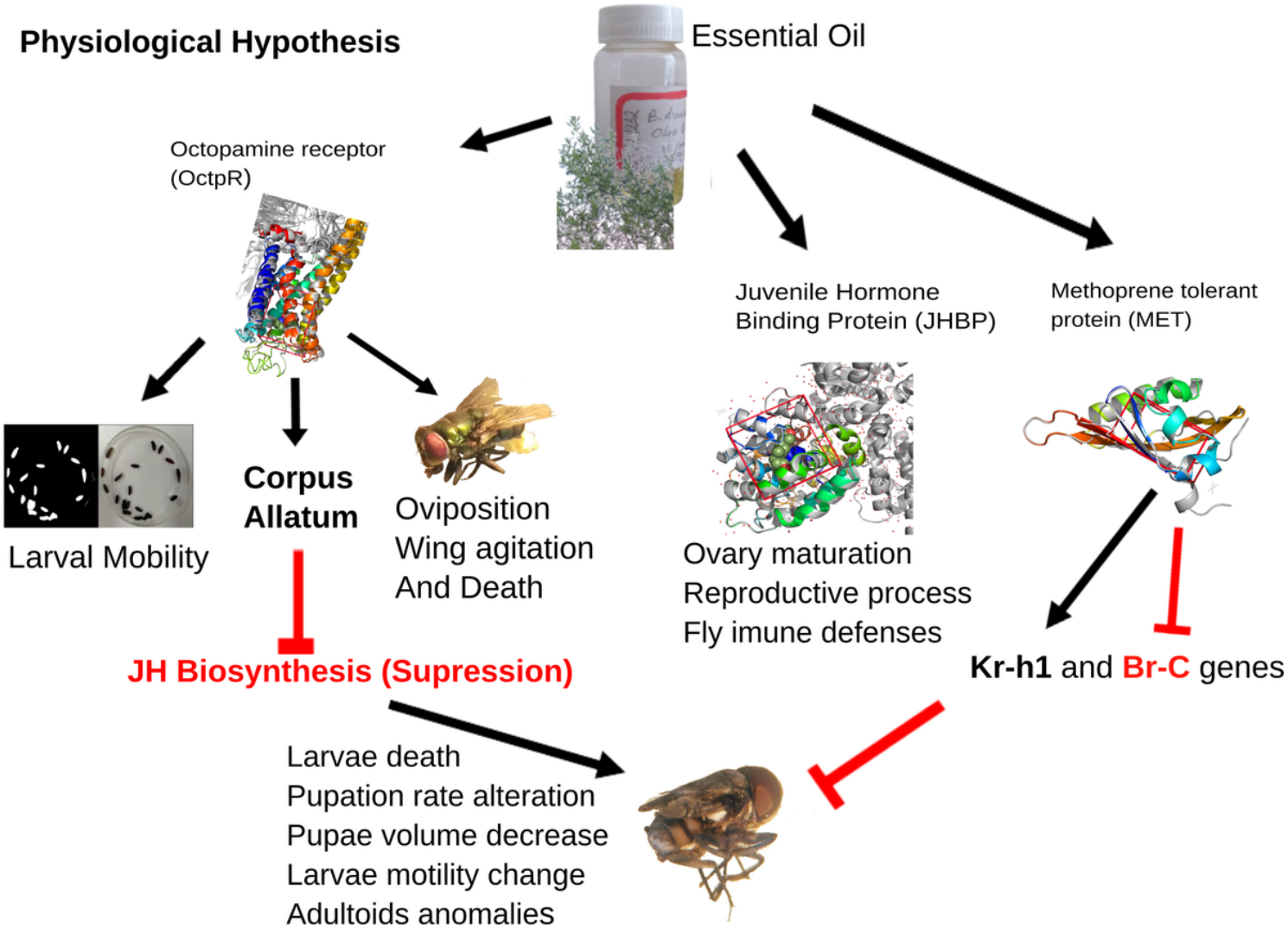

Figure 8

The physiological hypothesis of essential oils' action on blowfly metabolism. Diagram based on the computational and experimental results. Black arrow point induction and red line suppression.

Supplementary Files

This is a list of supplementary files associated with this preprint. Click to download.

- FiguresSupplementaryMaterials.zip
- NaturalcompoundsDataset.xlsx
- SupplementaryMaterialversion3.docx
- VideosSupplementaryMaterials.zip